



## OPEN

## SUBJECT AREAS:

ENVIRONMENTAL  
SCIENCES

SUSTAINABILITY

CLIMATE-CHANGE POLICY

# Spatial Simulation of Land Use based on Terrestrial Ecosystem Carbon Storage in Coastal Jiangsu, China

Xiaowei Chuai<sup>1</sup>, Xianjin Huang<sup>1,2</sup>, Wanjing Wang<sup>3</sup>, Changyan Wu<sup>1</sup> & Rongqin Zhao<sup>4</sup>Received  
21 January 2014Accepted  
23 June 2014Published  
11 July 2014

Correspondence and requests for materials should be addressed to X.W.C. (chuaixiaowei@163.com) or X.J.H. (hxj369@nju.edu.cn)

<sup>1</sup>School of Geographic & Oceanographic Sciences, Nanjing University, Nanjing 210023, Jiangsu Province, China, <sup>2</sup>Land Development and Consolidation Technology Engineering Center of Jiangsu Province, Nanjing 210023, Jiangsu Province, China, <sup>3</sup>College of Environmental Sciences and Engineering, Peking University, Beijing 100871, China, <sup>4</sup>North China University of Water Resources and Electric Power, Zhengzhou, Henan 450011, Henan Province, China.

This paper optimises projected land-use structure in 2020 with the goal of increasing terrestrial ecosystem carbon storage and simulates its spatial distribution using the CLUE-S model. We found the following: The total carbon densities of different land use types were woodland > water area > cultivated land > built-up land > grassland > shallows. Under the optimised land-use structure projected for 2020, coastal Jiangsu showed the potential to increase carbon storage, and our method was effective even when only considering vegetation carbon storage. The total area will increase by reclamation and the original shallows will be exploited, which will greatly increase carbon storage. For built-up land, rural land consolidation caused the second-largest carbon storage increase, which might contribute the most as the rural population will continue to decrease in the future, while the decrease of cultivated land will contribute the most to carbon loss. The area near the coastline has the greatest possibility for land-use change and is where land management should be especially strengthened.

Land-use change is a major driver of terrestrial ecosystem carbon storage<sup>1</sup>. Changes of land-use type from high- to low-vegetation biomass release carbon into the atmosphere. This not only reduces carbon storage in vegetation directly<sup>2</sup> but can also determine the amount of vegetation residue returned to the soil, which is the main source of soil carbon storage (SOC)<sup>3–5</sup>. As high-vegetation biomass, woodland usually has high SOC densities compared with other land-use types<sup>6,7</sup>. Changes from woodland to other land uses usually release carbon from soil, especially the upper soil<sup>8</sup>. However, there are studies showing cultivated land with higher SOC densities than woodland<sup>9</sup>, which may be attributed to the use of organic fertiliser and straw that is returned to the soil. Because vegetation and soil carbon densities vary with land-use type, land-use change can affect carbon storage, although this may take a long time for soil<sup>10</sup>. With continued urbanisation, increasing areas of cultivated land, woodland and wetland have been converted to built-up land, which greatly influences carbon storage in terrestrial ecosystems. The impact on carbon balance of land-use and land-cover changes in terrestrial ecosystems has become a focus of global change research in recent decades<sup>11</sup>.

Many scholars have proposed increasing carbon storage by adjusting the land-use structure, which appeared to be an effective plan. Lai (2010)<sup>12</sup> and Chuai et al. (2013)<sup>1</sup> optimised land-use structure to increase carbon storage at the national and provincial scales in China, respectively, finding that such measures can help China reduce carbon emissions effectively. Zhong et al. (2006)<sup>13</sup> optimised land-use readjustment to reduce carbon storage loss in Cuiyuan Village in Hubei Province, China. Coastal zones are natural transition regions between terrestrial ecosystems and ocean ecosystems. These zones usually have marine characteristics, such as wetlands, shallows and salt pans along coastlines. Moreover, 60% of the world's population is concentrated in coastal areas, where there is typically a highly developed economy with frequent land-use change<sup>14,15</sup>. The carbon emissions caused by such change are greater than in inland areas<sup>1,13</sup>. Some studies have targeted carbon storage variations brought about by land-use change in coastal regions, but only in single ecosystems. These studies involved carbon emissions caused by deforestation<sup>16</sup> and degradation of wetlands<sup>17,18</sup>. However, no land-use structure optimisation based on high carbon storage has been performed for coastal regions. Furthermore, all research examining measures to increase carbon storage in other regions has only performed optimisation from the aspect of land-use area. Where will the greatest land-use changes be? Which regions will have greater pressure to increase carbon storage, and what will be the future spatial distribution of the principal land-use transfers? All these questions

Table 1 | Carbon densities of different land-use types in coastal Jiangsu (t/km<sup>2</sup>)

| Carbon density | Land use type   |          |         |            |         |               |
|----------------|-----------------|----------|---------|------------|---------|---------------|
|                | Cultivated land | Woodland | Wetland | Water area | Shallow | Built-up land |
| Vegetation     | 543             | 3360     | 488     | 0          | 107     | 482           |
| Soil           | 8560            | 8710     | 6040    | 9090       | 5410    | 8267          |
| Total          | 9103            | 12070    | 6528    | 9090       | 5517    | 8750          |

remain unanswered, so the study of land-use structure optimisation based on terrestrial ecosystem carbon storage and its spatial simulation in coastal regions is necessary and meaningful.

In this study, we use land-use data, soil sample data, and data related to vegetation carbon densities and developmental policies in the coastal region of Jiangsu Province. Based on these data, this work investigates the carbon densities of different land-use types, establishes a land-use structure optimisation model to maximize terrestrial ecosystem carbon storage, simulates the spatial distribution of the optimised land use structure in 2020 by CLUE-S model, and analyzes the main land transfer types that can affect carbon storage and their spatial distributions between 2010–2020.

## Results

**Carbon densities of various land uses and changes.** Table 1 shows that carbon densities vary widely with land-use type in coastal areas of Jiangsu Province. Differences in vegetation carbon densities were great, with a highest density of 3,360 t/km<sup>2</sup> and a lowest density of zero. The soil carbon density ranged from 5,410 to 9,090 t/km<sup>2</sup>. Woodlands have greater total carbon densities relative to other land-use types and, in our study, woodland had the highest vegetation carbon density and second-highest soil carbon density. The total carbon density of cultivated land was similar to that of the water area, both of which were much higher than that of wetland; neither the vegetation nor soil of wetland had high carbon densities in our coastal study area. The carbon densities of shallows were the lowest compared with other land-use types, but built-up land had high densities, only slightly lower than cultivated land and water area.

According to the total carbon density values for different land-use types, a transfer from cultivated land always resulted in carbon storage loss, except for the transfer to woodland. Transfer from woodland, with the highest carbon density, to any other land-use type caused high carbon loss. This was especially so with the transfer to shallow soil, with 6,553 t carbon loss per km<sup>2</sup>, the maximum change

observed. Wetland loss always increased carbon storage, except when a transfer was made to shallow soil. Transfers from water area and built-up land to cultivated land and woodland increased carbon storage. Transfer from shallow soil, with the lowest carbon density, to any other land-use type increased carbon storage.

### Effect of optimised land-use structure on increased carbon storage.

As indicated in Table 2, the total carbon storage in coastal Jiangsu in 2010 was  $29,759.07 \times 10^4$  t. Within ten years, variations in carbon storage mainly resulted from vegetation changes in new land-use areas. Carbon in soil changes slowly and is primarily determined by the previous land-use type, so we only calculated the carbon storage change due to vegetation. Thus, the regional total carbon storage will reach  $29,938.75 \times 10^4$  t in 2020 under the optimised land-use structure proposed in this paper. This optimal structure will increase carbon storage by  $179.68 \times 10^4$  t compared with the 2010 structure. A total of  $157.26 \times 10^4$  t of the calculated increased storage resulted from reclamation of the new increased area, consisting primarily of reclamation as cultivated land ( $108.40 \times 10^4$  t). The remaining  $22.41 \times 10^4$  t of increased carbon storage resulted from land-use structure adjustment of the original 2010 land areas. Without considering the new increased land area, most ecological land area will increase, especially the water area, which will increase by 893.53 km<sup>2</sup>. However, because we only consider vegetation carbon storage and the water area has no vegetation, any increases of that area will not increase carbon storage. Wetland and woodland will increase by 358.39 and 85.51 km<sup>2</sup>, respectively, but because the vegetation carbon density of woodland is much higher than that of wetland, the increased woodland area can increase carbon storage more. To meet the demand for economic development, the decreasing trend in cultivated land area cannot readily be stopped and will lead to  $21.86 \times 10^4$  t carbon loss. The expansion of built-up land will be controlled effectively, with only

Table 2 | Changes of optimised land-use structure and carbon storage between 2010 and 2020

| Land use type                      | 2010     | 2020              |                          | Changes (2010–2020) |                          |                                   |
|------------------------------------|----------|-------------------|--------------------------|---------------------|--------------------------|-----------------------------------|
|                                    |          | No increased area | Including increased area | No increased area   | Including increased area | Reclamation of new increased area |
| Land area (km <sup>2</sup> )       |          |                   |                          |                     |                          |                                   |
| Cultivated land                    | 24325.31 | 23922.78          | 25919.04                 | -402.53             | 1593.73                  | 1996.26                           |
| Woodland                           | 311.30   | 396.81            | 396.81                   | 85.51               | 85.51                    | 0.00                              |
| Wetland                            | 520.47   | 878.86            | 1340.27                  | 358.39              | 819.80                   | 461.41                            |
| Water area                         | 2300.61  | 3194.14           | 3194.14                  | 893.53              | 893.53                   | 0.00                              |
| Shallow                            | 1149.66  | 0.00              | 710.81                   | -1149.66            | -438.85                  | 710.81                            |
| Built-up land                      | 4771.11  | 4985.87           | 5374.76                  | 214.76              | 603.65                   | 388.89                            |
| Total                              | 33378.46 | 33378.46          | 36935.83                 | 0.00                | 3557.37                  | 3557.37                           |
| Carbon storage (10 <sup>4</sup> t) |          |                   |                          |                     |                          |                                   |
| Cultivated land                    | 22143.33 | 22121.47          | 22229.87                 | -21.86              | 86.54                    | 108.40                            |
| Woodland                           | 375.74   | 404.47            | 404.47                   | 28.73               | 28.73                    | 0.00                              |
| Wetland                            | 339.76   | 357.25            | 379.77                   | 17.49               | 40.01                    | 22.53                             |
| Water area                         | 2091.25  | 2091.25           | 2091.25                  | 0.00                | 0.00                     | 0.00                              |
| Shallow                            | 634.27   | 621.97            | 629.57                   | -12.30              | -4.70                    | 18.74                             |
| Built-up land                      | 4174.72  | 4185.07           | 4203.82                  | 10.35               | 29.10                    | 7.61                              |
| Total                              | 29759.07 | 29781.49          | 29938.75                 | 22.41               | 179.68                   | 157.27                            |



214.76 km<sup>2</sup> increased area, which can increase carbon storage by  $10.35 \times 10^4$  t in the form of vegetation.

To clearly analyse the carbon storage change caused by original land-use transfer without consideration of the new increased land area, we constructed a land-use and carbon storage transfer matrix between 2010 and 2020, based on the original study area in 2010. As indicated in Table 3, 2,236.13 km<sup>2</sup> land area will be transferred to other land use types, representing 7.18% of the entire land area in 2010. All original shallows will be transferred, with a large area of 1,149.66 km<sup>2</sup>, accounting for 51% of the entire transferred area. This can increase vegetation carbon storage by  $29.05 \times 10^4$  t. The main transfers are to wetland, water area, built-up land and cultivated land, with vegetation carbon storage changes of 12.33,  $-3.14$ , 11.68 and  $8.47 \times 10^4$  t, respectively. Cultivated land will contribute 786.95 km<sup>2</sup> land area for transitions. This represents 35% of the entire transferred area and will decrease carbon storage by  $7.37 \times 10^4$  t, with transitions to built-up land and water areas contributing most to this decrease. Transitions to woodland will most inhibit this decrease. Because of the consolidation of rural residential land, some built-up land has the potential to be converted to cultivated land (190.24 km<sup>2</sup>) and water area (93.92 km<sup>2</sup>), but this would weakly increase carbon storage, because water area has no vegetation. No decreases were allowed for woodland, wetland or water area because of their high carbon density to maximum carbon storage ratio.

**Spatial distribution of land-use conversion between 2010 and 2020 and reclamation of new increased area.** According to the effective CLUE-S model we tested, we produced spatial distributions of optimised land-use structure. To discover where clear land-use transfer will occur, what the principal transfer types will be, and which regions will have greater pressure to increase carbon storage, we also produced a land-use transfer map comparing 2010 and 2020. Using this and the reclamation plan for the new increased area, we constructed Fig. 1. The figure shows that coastline regions have a strong potential for land transition, exhibiting concentrated distributions for both the original land area and the new increased area. Reclamation of the new increased area will mainly occur along the southern coastline where there are obvious sedimentation effects. Inland regions have dispersed distributions, and transitions will mainly occur southwest of Yancheng and Nantong and north of Lianyungang, regions where cities and towns are mostly located.

Except for the new increased area, we established six buffer areas with distances to the coastline of 0–10 km, 10–20 km, 20–40 km, 40–60 km, 60–80 km and 80–100 km, to show regional differences

in land transitions. As indicated in Table 4, the highest percentage of transferred land relative to the total buffer area was in buffer area 1. This value was 26.9%, much higher than in other buffer areas, with a total area of 1,518.26 km<sup>2</sup>, representing 67.32% of the entire transferred land area. This indicates that land in the 0–10 km range from the coast has the highest probability of transfer. The main transfer types include cultivated land to water area; shallow soil to wetland, built-up land, water area and cultivated land; and cultivated land to built-up land. In buffer 2, the percentage decreased sharply to 4.08%, with main transfers of cultivated land to water area, built-up land and wetland. Buffer 3 showed the lowest percentage and smallest absolute transfer area at 98.59 km<sup>2</sup>. Buffers 4, 5 and 6 showed increasing percentages from 1.73% to 9.13%, with absolute areas from 137.53 to 106.26 km<sup>2</sup>. The much higher value of 9.13% in buffer 6 is attributable to widespread water area there; the nearby land is under great pressure to be replaced by water area.

Without consideration of soil organic carbon, we produced a map of vegetation carbon density changes in Fig. 2 to show the spatial distribution of carbon sinks or sources generated by land-use change. This shows that the reclamation of the new increased area will strongly enhance carbon storage because the original sandy beach will be covered by vegetation, especially in the case of reclamation to cultivated land. For the original land area transitions, most transitions near the coastline have great potential to increase carbon storage, especially in the central and south regions. Part of the northern coastline is under pressure to lose carbon storage capacity, because of water area expansion. The transition of cultivated land to built-up land in those areas will also lead to carbon loss. For inland districts, most of the transferred area will enhance carbon storage. The regions of carbon loss are mainly located in western Yancheng. This is primarily caused by the transition of cultivated land to water area.

## Discussion

Land-use change caused by human activities is a main driver of modifications to terrestrial ecosystem carbon storage<sup>1</sup>. Coastal regions usually have highly developed economies, which drive frequent land-use changes<sup>14,15</sup>. Using land-use type maps from 2005 and 2010, vegetation-type maps, soil sample data, and other empirical data related to carbon densities for different terrestrial ecosystems, and based on a linear programming model and the CLUE-S model, we examined carbon densities of both vegetation and soil for various land-use types. Based on these carbon densities, we optimised land-use structure in 2020 based on maximum carbon storage in terrestrial ecosystems and simulated its spatial distribution in coastal Jiangsu.

**Table 3 | Land use and carbon storage transfer matrix between 2010 and 2020 in coastal Jiangsu**

| 2020   |                 |          |         |            |         |               |          |
|--|-----------------|----------|---------|------------|---------|---------------|----------|
| 2010   | Cultivated land | Woodland | Wetland | Water area | Shallow | Built-up land | Total    |
| <b>Land use transfer (km<sup>2</sup>)</b>                    |                 |          |         |            |         |               |          |
| Cultivated land  | 23538.36        | 71.43    | 34.40   | 480.16     | 0.00    | 200.96        | 24325.31 |
| Woodland   | 0.00            | 311.30   | 0.00    | 0.00       | 0.00    | 0.00          | 311.30   |
| Wetland  | 0.00            | 0.00     | 519.99  | 0.00       | 0.00    | 0.48          | 520.47   |
| Water area   | 0.00            | 0.96     | 0.00    | 2299.65    | 0.00    | 0.00          | 2300.61  |
| Shallow  | 194.18          | 0.00     | 323.67  | 320.41     | 0.00    | 311.40        | 1149.66  |
| Built-up land  | 190.24          | 13.12    | 0.80    | 93.92      | 0.00    | 4473.03       | 4771.11  |
| Total  | 23922.78        | 396.81   | 878.86  | 3194.14    | 0.00    | 4985.87       | 33378.46 |
| <b>Vegetation carbon storage transfer (10<sup>4</sup> t)</b> |                 |          |         |            |         |               |          |
| Cultivated land  | 0.00            | 20.12    | -0.19   | -26.07     | 0.00    | -1.23         | -7.37    |
| Woodland   | 0.00            | 0.00     | 0.00    | 0.00       | 0.00    | 0.00          | 0.00     |
| Wetland  | 0.00            | 0.00     | 0.00    | 0.00       | 0.00    | 0.00          | 0.00     |
| Water area   | 0.00            | 0.32     | 0.00    | 0.00       | 0.00    | 0.00          | 0.32     |
| Shallow  | 8.47            | 0.00     | 12.33   | -3.43      | 0.00    | 11.68         | 29.05    |
| Built-up land  | 1.16            | 3.78     | 0.00    | -4.53      | 0.00    | 0.00          | 0.41     |
| Total  | 9.63            | 24.22    | 12.14   | -34.03     | 0.00    | 10.45         | 22.41    |

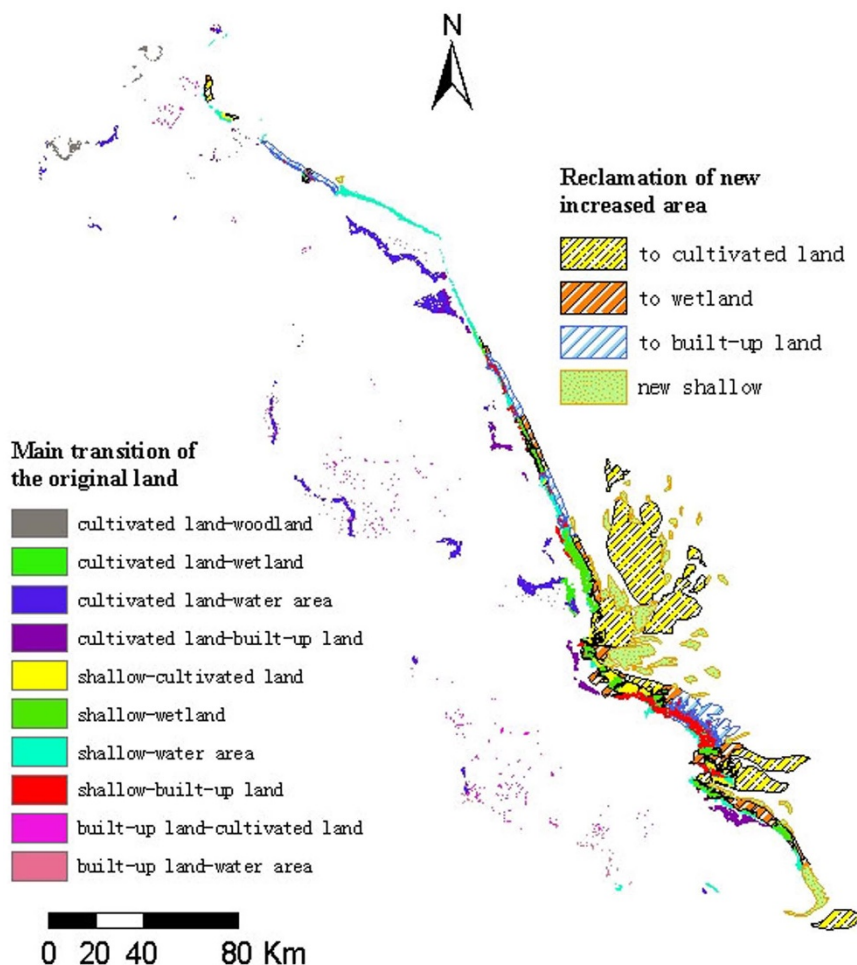


**Figure 1** | Spatial distribution of land-use transfer between 2010 and 2020. Map created using ArcMap 9.3 software. (Environmental Systems Resource Institute (ESRI), Redlands, CA, USA).

Between 2010 and 2020, we used only vegetation carbon storage to analyse the effects of the optimised land-use structure on increasing carbon storage. Because carbon in soil changes slowly, possibly occurring over periods longer than ten years<sup>10</sup>, carbon storage for new land-use types is mostly determined by previous types. We also assumed that no land-use types gain or lose carbon over time. The only changes in carbon storage considered were those resulting from the conversion of one land-use type to another. Our study area is mainly covered by crops and wetland vegetation. Crop vegetation covers most of the area, and it has relatively stable growth because of agricultural management. Wetland vegetation is mainly located along the coast, and large areas have been effectively protected by ecological protection zones<sup>19</sup>. Thus, vegetation growth status was not considered in our study,

Woodland had the highest carbon density in all regions, which can be explained by the fact that it always has high levels of biomass

sequestered as vegetation<sup>12</sup>. Moreover, woodlands create more residual vegetation, which can also enhance carbon storage in soil<sup>4</sup>. Although lacking vegetation, water areas also showed high SOC densities. This is likely attributed to water transport mechanisms that can collect organic carbon from other areas and accumulate it in silt under the water<sup>20</sup>, as well as to long-term flooding conditions that reduce decomposition rates<sup>7</sup>. The carbon density of cultivated land was only slightly less than that of water area, which can be explained by the fact that cultivated land has a greater vegetation biomass than all other land-use types except woodland. For soils, the effects of returned crop residues and straw, long-term use of organic fertilisers, and flooding of paddy land in our study area can also enhance carbon storage<sup>21,22</sup>. Built-up land has a vegetation carbon density similar to wetlands. This is due to the high vegetation coverage rate in coastal Jiangsu. The high soil carbon density agrees with the results of earlier studies<sup>23,24</sup> and can be explained by the multitude of soil carbon

**Table 4** | Comparison of transferred land in different buffer areas

| Buffer area code | Distance to coastline (km) | Transferred land accounts for total buffer area | Main transfer type (from high to low according to area)  |
|------------------|----------------------------|---|--|
| 1                | 0–10                       | 26.90%  | Cultivated land to water area, shallow to wetland, built-up land, water area and cultivated land, cultivated land to built-up land |
| 2                | 10–20                      | 4.08%   | Cultivated land to water area, built-up land and wetland   |
| 3                | 20–40                      | 1.03%   | Cultivated land to water area and woodland, built-up land to cultivated land   |
| 4                | 40–60                      | 1.73%   | Cultivated land to water area, built-up land to cultivated land  |
| 5                | 60–80                      | 3.54%   | Built-up land to cultivated land, cultivated land to water area and woodland   |
| 6                | 80–100                     | 9.13%   | Cultivated land to water area, built-up land to water area   |

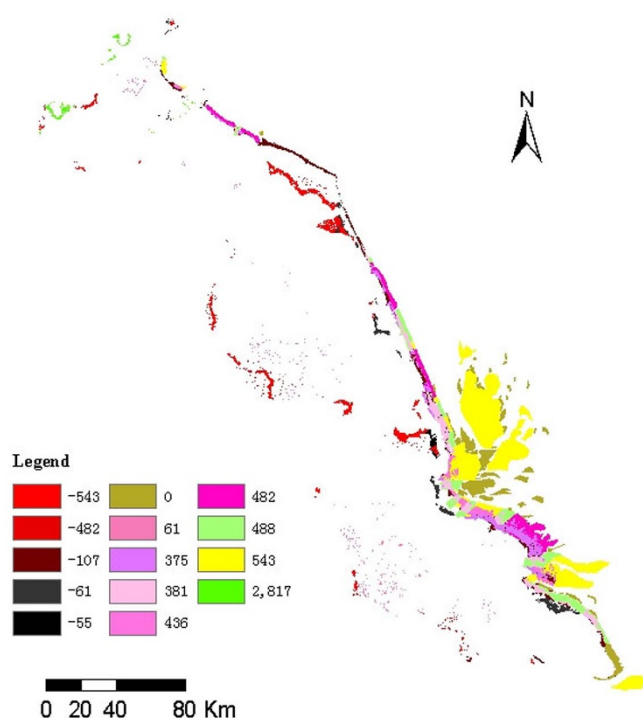


**Figure 2** | Spatial distribution of carbon density changes between 2010 and 2020 ( $t/km^2$ ). Map created using ArcMap 9.3.

sources in towns, including vegetation such as leaves, twigs and weeds, substantial amounts of household garbage, and organic waste produced by urban industries<sup>7</sup>. Additionally, soil in urban areas is generally compacted and sealed, which can prevent the release of soil carbon into the atmosphere, thereby reducing carbon decomposition and increasing its accumulation<sup>7</sup>. The carbon density of wetlands was relatively low. This contradicts earlier studies that showed higher carbon densities for wetlands compared with other terrestrial ecosystems, especially for soil<sup>25,26</sup>. This can be explained by the fact that wetlands in our area are mainly composed of halophytic vegetation and are located in coastal solonchak soil areas with high sand content. These soils do not favour the concentration of carbon in the soil<sup>27</sup>. Shallows have little vegetation coverage and are a weak carbon source, and the sand content in solonchak soil may be even higher than that in wetland areas, so shallows had the lowest carbon densities overall.

The reclamation of new increased area can greatly benefit carbon storage. Without considering the new increased area and the SOC of the entire area, we can increase carbon storage by  $22.41 \times 10^4$  t in coastal Jiangsu by adjusting the land-use structure. This can offset 1.88% and 1.05% of the carbon emissions resulting from increased regional energy consumption in 2005 and 2010<sup>24</sup>, respectively. If we fail to optimise and permit the land-use structure to change as it did in 2005–2010, many more ecological land-use types, such as cultivated land, woodland and wetland, will decrease sharply. Moreover, the expansion of built-up land will occur more rapidly. The much greater decrease of ecological land will lead to tremendous carbon loss from both vegetation and soil. The rapid expansion of built-up land will also lead to more anthropogenic carbon emissions. Because the principal activities of energy consumption are tied to certain types of such land, there are usually high carbon emissions from energy consumption. Putting limits on this land type can therefore obviously decrease carbon emissions from energy consumption<sup>12,28</sup>. Ecological lands can also provide benefits other than carbon storage, such as water conservation and flood control, erosion control, fuel, food, biodiversity and others<sup>29</sup>. Our study did not consider carbon changes due to soil. If there is sufficient time for the transferred land

to mature into another ecological land system, the optimised land structure will cause another  $314.18 \times 10^4$  t SOC increase, without consideration of the new increased area as a long-term effect. Some transition types in our optimised land-use structure that can lead to carbon loss may yield opposite effects, such as the transition of cultivated land to water area. Although this process will not be completely finished during the period 2010–2020, there will be real SOC changes to some extent during that decade, especially in the surface soil layer. Consequently, the actual increased carbon storage may be much greater than  $22.41 \times 10^4$  t from vegetation only. Furthermore, many land-use types currently undergoing natural succession can continue to accumulate carbon for a very long time<sup>30</sup>, because our analysis was based on the assumption that none of the land-use types gain or lose carbon over time. If vegetation is well protected, carbon storage in 2020 will increase because of the carbon sink effect of vegetation. Therefore, the optimised land use structure is effective, especially over the long-term.

The spatial distribution simulation indicated that the area near the coast had the greatest probability of land-use change. This is determined by the development policy for the coastal zone proposed by the provincial government. Thus, we should pay more attention to the near-coastal area. In addition to land-transfer type control, we can also adopt other means to increase carbon concentrations in this important region, including land management, tillage practices such as combined use of inorganic fertiliser and organic manure on cultivated land, and the application of a suitable crop rotation system<sup>31</sup>. The reclamation of sand beaches and shallows can produce most of the increased carbon storage, but we should pay attention to the protection of the ecological environment during the process of exploitation<sup>32</sup>. Because the rural population is declining, the demand for rural residences will shrink. Rural residential land will most likely be converted to cultivated land or other land types, and this represents a high potential for increasing carbon storage. Thus, we should strengthen rural land consolidation, which may contribute the most to increasing carbon storage in the future.

In summary, our study may be valuable to land managers and local governments, for we examined carbon storage capacities of different land use types. Our method can effectively increase carbon storage in coastal Jiangsu and can guarantee land-use demands for coastal economic and social development. Our spatial simulation analysis clarified the spatial distribution of land-transfer types, which can make spatial land management more targeted and effective. Therefore, this study can be highly beneficial to the ecological and sustainable development of coastal Jiangsu.

## Methods

**Study region.** The coastal region of Jiangsu faces the Yellow Sea to the east and the Yangtze River to the south. The study area encompasses the cities of Lianyungang, Yancheng and Natong (Fig. 3), with an area of  $3.3 \times 10^4$  km<sup>2</sup>, or 35% of Jiangsu's total land area. The area lies between  $31^{\circ}41'N$ – $35^{\circ}07'N$  and  $118^{\circ}24'E$ – $121^{\circ}55'E$ . The total length of the coastline is 954 km. In recent years, the economy has developed rapidly, with frequent land use changes<sup>14</sup>.

**Data sources.** The 100 m  $\times$  100 m grid land-use map was produced from Landsat Thematic Mapper data. The vegetation-type map was compiled using data from the 2000s and was able to effectively describe the most recent vegetation distribution in the study area. There were 7,797 soil samples obtained from a multi-purpose regional geochemical survey in Jiangsu Province from 2003 to 2007. Forest data were acquired from The Fifth Forest Resource Inventory in the province. Crop yield data were obtained from statistical yearbooks of the three coastal cities. Other empirical data were obtained from related research studies.

Spatial driving factor maps included population density, GDP density, elevation, and distances to main roads, cities, villages, ports, coastline, and main water lines. Population and GDP data were obtained from statistical yearbooks of the three coastal cities. A digital elevation model (DEM) was created based on Shuttle Radar Topography Mission data provided by the International Scientific Data Service Platform.

All figures (1–3) in our paper were generated by geographic information system mapping techniques.

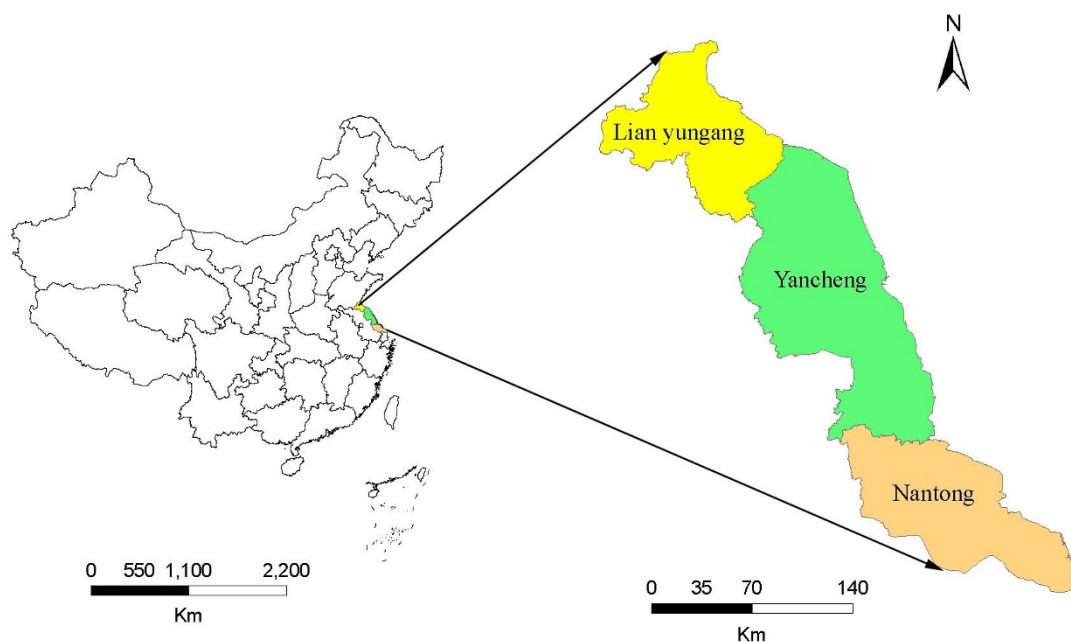


**Figure 3** | Location of study area. Map created using ArcMap 9.3.

**SOC densities for different land uses.** For each soil sample, the SOC density was calculated by the following equation:

$$SOCD = 1000 \times TOC \times \rho \times h, \quad (1)$$

where  $SOC$  represents SOC density,  $TOC$  is the soil organic carbon content (%),  $\rho$  is the bulk density, and  $h$  is the soil depth.

Geographic information system mapping techniques were used to produce soil sample distribution maps according to latitude and longitude. Kriging methods based on a spherical model were then used, and the sample point data were converted to polygon data covering the entire study area. Based on the land-use map of 2005, zonal statistics in ArcGIS 9.3 software (Environmental Systems Resource Institute (ESRI), Redlands, CA, USA) were used to compare soil carbon densities under various land uses.

#### Vegetation carbon densities for different land uses.

- 1) Woodland. This was calculated from biomass density and carbon content. According to related previous studies, the carbon content of trees is usually taken as 0.5<sup>33</sup>, and the calculations are shown below.

$$W = \frac{\sum_{ij} W_{ij} \times S_{ij}}{\sum_{ij} S_{ij}} \quad W_{ij} = B_{ij} \times 0.5 \quad B_{ij} = a + bV_{ij}, \quad (2)$$

where  $W$  is the average vegetation carbon density of woodland;  $W_{ij}$ ,  $S_{ij}$  and  $B_{ij}$  are the vegetation carbon density, woodland area and vegetation biomass densities for tree type  $i$  and tree-age  $j$ , respectively;  $V_{ij}$  is tree volume density; and  $a$  and  $b$  are constants obtained from the study of Xu et al. (2007)<sup>33</sup>, who established a linear regression equation between forest biomass and its volume, based on 2304 forest sample plots in China.

- 2) Cultivated land. Major crops in coastal Jiangsu include rice, wheat, corn, beans, potato, cotton, peanuts, rapeseed, sugar and vegetables. Here we calculate the crop vegetation carbon density according to cropland yield as shown below:

$$C = \frac{\sum_i C_i \times S_i}{\sum_i S_i} \quad C_i = \frac{P_i \times (1 - W_i) \times Y_i}{H_i \times S_i}, \quad (3)$$

where  $C$  is the average vegetation carbon density of cultivated land;  $C_i$  is the vegetation carbon density of crop type  $i$ ;  $S_i$  is the area of crop type  $i$ ; and  $P_i$ ,  $W_i$ ,  $Y_i$ , and  $H_i$  represent the crop yield, water content, ability to absorb carbon, and the economic coefficient of crop type  $i$ , respectively.  $S_i$  and  $P_i$  were obtained from statistical yearbooks of the three coastal cities, and values for  $W_i$ ,  $Y_i$  and  $H_i$  were acquired from the results of related research by Zhao (2011)<sup>34</sup>, who carried out a similar study in Nanjing, Jiangsu.

- 3) Other land. For wetland, biomass data for various types of vegetation are quoted from the research of Zong et al. (1992)<sup>35</sup>, who studied the biomass of saltwater vegetation and sand vegetation on the coast of Jiangsu Province. Shallows can be divided into *Artemisia halodendron*-dominated beaches, marshes dominated by *Spartina* and bare beaches. Therefore, according to

the vegetation type and area, the vegetation carbon density of shallows can be calculated. The vegetation carbon density of trees and grass scattered among built-up land was determined according to the vegetation coverage rate and the mean values of tree and grass carbon density. We defined the vegetation carbon density of water area as zero, because it has almost no vegetation coverage.

**Land-use structure optimisation.** A linear programming model was selected to optimise land-use structure. This model includes the establishment of a target function (Equation 4) and constraint conditions.

$$T = \sum_{i=1}^n A_i(V_i + S_i) = \max \quad i = 1, 2, 3, \dots, n, \quad (4)$$

where  $T$  is the regional total carbon storage of the terrestrial ecosystem;  $A_i$  is the area of land-use type  $i$ ; and  $V_i$  and  $S_i$  are the carbon densities of the vegetation and soil of land-use type  $i$ , respectively.

We established constraint conditions for six variables as follows: cultivated land  $X_1$ , woodland  $X_2$ , wetland (with herbaceous vegetation)  $X_3$ , water area  $X_4$ , shallows  $X_5$ , and built-up land  $X_6$ . Here we set 2010 as the initial year and 2020 as the targeted prediction year.

About a third of the coastline in the study area suffered erosion<sup>36</sup>, mainly within Lianyungang. The remaining area suffered deposition effects. This effect was much more obvious than erosion, and it expanded the total land area annually. The erosion approached the coastal levee. This will weaken or stop the erosion effect<sup>37</sup>, and the total study area will continue to increase in the future. In contrast to our previous study<sup>24</sup>, here we considered the land reclamation plans of local government. The affected land is principally along the coastline and offshore sand beaches, which will mainly be treated by engineering efforts. Thus, we predict that the total area will reach 36,935.83 km<sup>2</sup> by 2020:

$$\sum_{i=1}^6 X_i = 36,935.83 \quad X_i \geq 0 \quad (5)$$

To guarantee local food self-sufficiency, 21,925.19 km<sup>2</sup> of cultivated land will be needed, which we consider a low value. According to the land consolidation potential of rural residential and land reclamation plans, we predict that cultivated land can reach 25,919.75 km<sup>2</sup> by 2020, which we consider a high value.

$$21,925.19 \leq X_1 \leq 25,919.75 \quad (6)$$

Woodland should be strictly protected, such that its area in 2020 should at least be higher than in 2010 (311.3 km<sup>2</sup>). According to the 12th Five-Year Plan of forestry development planning and the demands of ecological construction, the area of woodland will increase by 85.51 km<sup>2</sup> in 2020 over that in 2010 with effective implementation. The constraint conditions are established as:

$$311.3 \leq X_2 \leq 396.81 \quad (7)$$

Considering Yancheng coastal agricultural development planning, we predicted in our previous study<sup>26</sup> that wetland will reach at least 687.14 km<sup>2</sup> by 2020, because of



planted grass. According to the land reclamation plan, part of the existing shallows and new increased sand beaches will be reclaimed as wetland, which would increase the area by 653.13 km<sup>2</sup>. Wetland should be strictly protected because of its significant carbon sink effect, so we establish the constraint conditions as follows:

$$X_3 \geq 1,340.27 \quad (8)$$

According to water conservancy development planning of the three coastal cities, at least 94.3 km<sup>2</sup> of new area will be needed compared with 2010, which we consider a low value. The increased water area is mainly converted from wetland, and the total water area will reach 2,896.35 km<sup>2</sup> according to the rate of increase between 2005 and 2010. We consider this a high value, because wetland will be protected strictly as stated above. Moreover, according to the reclamation plan, another 297.19 km<sup>2</sup> of existing shallows will be converted to water area. Therefore, we should add this to the low and high water-area values above:

$$2,692.69 \leq X_4 \leq 3,194.14 \quad (9)$$

According to the reclamation plan, original shallow land in 2010 will be entirely converted to other land-use types. However, another 710.81 km<sup>2</sup> of new increased shallows will be present, owing to natural and artificial boosting of the deposition effect:

$$X_5 = 710.81 \quad (10)$$

According to population, per capita living space and land demands for traffic, at least 4,855.88 km<sup>2</sup> of built-up land will be needed in 2020, which we consider a low value. A high value is that used in land-use planning in Jiangsu Province (5,274.49 km<sup>2</sup>), which mainly considers the demands of economic development. According to the land reclamation plan, another 518.88 km<sup>2</sup> of built-up land will be needed, mainly for harbour construction, which will be reclaimed from existing shallows and the new increased sand beaches. Thus, we must add 518.88 km<sup>2</sup> to the high and low values:

$$5,374.76 \leq X_6 \leq 5,793.37 \quad (11)$$

**Spatial distribution simulation of optimised land-use structure.** We selected the CLUE-S model to perform the spatial distribution simulation of the optimised land-use structure. This simulation typically considers the following: (1) Land-use requirements (demand). For the various land-use types, these are calculated with the linear programming model described above. (2) Spatial restrictions. We chose major natural reserves as restrictions. (3) Land-use type conversion settings. According to the land-use transfer situation and model simulation accuracy, values of conversion elasticity for different land-use types were set as follows: cultivated land 0.5, woodland 0.6, wetland 0.3, water area 0.4, shallows 0.5, and built-up land 0.8. We set 2005 as the initial year and 2010 as the target year to test the accuracy of the CLUE-S model. The model passed the ROC and Kappa index tests well, and it was able to simulate land-use spatial distributions in 2020.

1. Chuai, X. W. *et al.* Land use structure optimization based on carbon storage of terrestrial ecosystems in different regions of China. *Environ Sci Policy* **25**, 50–61 (2013).
2. Muñoz-Rojas, M., De la Rosa, D., Zavala, L. M., Jordán, A. & Anaya-Romero, M. Changes in land cover and vegetation carbon stocks in Andalusia, Southern Spain (1956–2007). *Sci Total Environ* **409**, 2796–2806 (2011).
3. Dang, Y. A. *et al.* Climate and Land use controls on soil organic carbon in the Loess Plateau region of China. *Plos One* **9**, 1–11 (2014).
4. Jaiarree, S. *et al.* Soil organic carbon loss and turnover resulting from forest conversion to Maize fields in Eastern Thailand. *Pedosphere* **21**, 581–590 (2011).
5. Zhang, J., Wang, X. J. & Wang, J. P. Impact of land use change on profile distributions of soil organic carbon fractions in the Yanqi Basin. *Catena* **115**, 79–84 (2014).
6. Xi, X. H. *et al.* Multi-purpose regional geochemical survey and soil carbon reserves problems: examples of Jiangsu, Henan, Sichuan, Jilin provinces and Inner Mongolia. *Quatern Sci* **28**, 58–67 (2008). (in Chinese).
7. Chuai, X. W. *et al.* Spatial variability of soil organic carbon and comprehensive analysis of related factors in Jiangsu Province, China. *Pedosphere* **22**, 404–414 (2012).
8. Puget, P., Lal, R., Izaurralde, C., Post, M. & Owens, L. Stock and distribution of total and corn-derived soil organic carbon in aggregate and primary particle fractions for different land use and soil management practices. *Soil Sci* **170**, 256–279 (2005).
9. Jiao, J. G. *et al.* Land use and soil organic carbon in China's village landscapes. *Pedosphere* **20**, 1–14 (2010).
10. Wang, Y. G. *et al.* Effects of Land use/Land cover change on carbon storage in Manas River Watershed over the past 50 Years. *J Nat Res* **28**, 994–1006 (2013). (in Chinese).
11. Houghton, R. A. Revised estimates of the annual net flux of carbon to the atmosphere from changes in land use and land management. 1850–2000, *Tellus B* **55**, 378–390 (2003).
12. Lai, L. Carbon emission effect of land use in China. Ph.D. Dissertation, Nanjing: Nanjing University, pp.45 (2010). (in Chinese).

13. Zhong, X. B., Yu, G. M., He, G. S. & Lu, D. Carbon storage loss during land readjustment and optimization of ecological compensation. *Chin J Ecol* **25**, 303–308 (2006). (in Chinese).
14. Yao, H. Characterizing land use changes in 1990–2010 in the coastal zone of Nantong, Jiangsu province, China. *Ocean Coast Manage* **71**, 108–115 (2013).
15. Ellis, J. T., Spruce, J. P., Swann, R. A., Smoot, J. C. & Hilbert, K. W. An assessment of coastal land-use and land-cover change from 1974–2008 in the vicinity of Mobile Bay, Alabama. *J Coast Conserv* **15**, 139–149 (2011).
16. Godoy, F. L. *et al.* Deforestation and CO<sub>2</sub> emissions in coastal Tanzania from 1990 to 2007. *Environ Conserv* **39**, 62–71 (2012).
17. Kauffman, J. B., Heider, C., Norfolk, J. & Payton, F. Carbon stocks of intact mangroves and carbon emissions arising from their conversion in the Dominican Republic. *Ecol Appl* **24**, 518–527 (2014).
18. Delaune, R. D. & White, R. J. Will coastal wetlands continue to sequester carbon in response to an increase in global sea level? A case study of the rapidly subsiding Mississippi river deltaic plain. *Climatic Change* **110**, 297–314 (2012).
19. Chen, H. Q. The characteristics and the protection of the coastal wetland resources in Jiangsu. *Ecol Econ* 195–198 (2003). (in Chinese).
20. Eatherall, A., Naden, P. S. & Cooper, D. M. Simulating carbon flux to the estuary: The first step. *Sci Total Environ* **210**, 519–533 (1998).
21. Adiku, S. G. K., Narh, S., Jones, J. W., Laryea, K. B. & Dowuona, G. N. Short-term effects of crop rotation, residue management, and soil water on carbon mineralization in a tropical cropping system. *Plant Soil* **311**, 29–38 (2008).
22. Lee, S. B., Lee, C. H., Jung, K. Y., Do, P. K. & Lee, D. Changes of soil organic carbon and its fractions in relation to soil physical properties in a long-term fertilized paddy. *Soil Till Res* **104**, 227–232 (2009).
23. Sun, Y. L., Ma, J. H. & Li, C. Contents and densities of soil organic carbon in urban soils in different function areas of Kaifeng. *Sci Geogr Sin* **29**, 124–128 (2009). (in Chinese).
24. Chuai, X. W. Carbon source/sink caused by land use changes in coastal regions—The case study of coastal region in Jiangsu Province. Ph.D. Dissertation, Nanjing: Nanjing University, pp.45 (2013). (in Chinese).
25. Hansen, V. D. & Nestlerode, J. A. Carbon sequestration in wetland soils of the northern Gulf of Mexico coastal region. *Wet Ecol Manag* **22**, 289–303 (2014).
26. Mcleod, E. *et al.* A blueprint for blue carbon: toward an improved understanding of the role of vegetated coastal habitats in sequestering CO<sub>2</sub>. *Front Ecol Environ* **9**, 552–560 (2011).
27. Jens, L., Seraina, B. & Jürg, F. Carbon stocks in Swiss agricultural soils predicted by land-use, soil characteristics, and altitude. *Agr Ecosyst Environ* **105**, 255–266 (2005).
28. Zhao, R. Q., Huang, X. J., Zhong, T. Y. & Peng, J. W. Carbon footprint of different industrial spaces based on energy consumption in China. *J Geogr Sci* **21**, 285–300 (2011).
29. Konarska, K. M., Sutton, P. C. & Castellon, M. Evaluating scale dependence of ecosystem service valuation: A comparison of NOAA AVHRR and Landsat TM datasets. *Ecol Econ* **41**, 491–507 (2002).
30. Luysaert, S. *et al.* Old-growth forests as global carbon sinks. *Nature* **455**, 213–215 (2008).
31. Campbell, C. A. & Zentner, R. P. Soil organic-matter as influenced by rotations and fertilization. *Soil Sci Soc Am J* **57**, 1034–1040 (1993).
32. Shen, Y. M., Feng, N. H., Zhou, Q., Liu, Y. M. & Chen, Z. Y. The status and its influence of reclamation on Jiangsu coast. *Mar Sci* **30**, 39–43 (2006). (in Chinese).
33. Xu, X. L., Cao, M. K. & Li, K. R. Temporal-spatial dynamics of carbon storage of forest vegetation in China. *Prog Geogr* **26**, 1–10 (2007). (in Chinese).
34. Zhao, R. Q. Carbon cycle of urban eco-economic system and its regulation through land use control: A case study of Nanjing city. Ph.D. Dissertation, Nanjing: Nanjing University, pp.54 (2011). (in Chinese).
35. Zong, S. X. *et al.* A study of the biomass and energy of salt vegetation and sand vegetation along the coast of Jiangsu Province. *J Plant Res Environ* **1**, 25–30 (1992). (in Chinese).
36. Dai, Y. N. & Peng, J. G. Fragility evaluation for the eco-environment of the coastal zone in Jiangsu. *J Mar Sci* **27**, 79–82 (2009). (in Chinese).
37. Cai, Z. J. & Wu, S. L. Remote sensing analysis of the coastline development in Jiangsu Province. *Remote Land Resour* **3**, 20–23 (2002). (in Chinese).

## Acknowledgments

This research was supported by the Clean Development Mechanism (CDM) projects of China (No.1214073 and No. 2012065), the Priority Academic Program Development of Jiangsu Higher Education Institutions, and the National Natural Science Foundation of China (No.41301633).

## Author contributions

X.H. initiated the concept of the study. X.H. and C.X. designed the research. C.X. conducted statistical analysis and drafted the manuscript. W.W., W.C. and Z.R. provided strategic advice and comments on the manuscript.

## Additional information

**Competing financial interests:** The authors declare no competing financial interests.



**How to cite this article:** Chuai, X.W., Huang, X.J., Wang, W.J., Wu, C.Y. & Zhao, R.Q. Spatial Simulation of Land Use based on Terrestrial Ecosystem Carbon Storage in Coastal Jiangsu, China. *Sci. Rep.* 4, 5667; DOI:10.1038/srep05667 (2014).



This work is licensed under a Creative Commons Attribution-NonCommercial-NoDerivs 4.0 International License. The images or other third party material in

this article are included in the article's Creative Commons license, unless indicated otherwise in the credit line; if the material is not included under the Creative Commons license, users will need to obtain permission from the license holder in order to reproduce the material. To view a copy of this license, visit <http://creativecommons.org/licenses/by-nc-nd/4.0/>